

# Test Results of LARP 3.6 m Nb<sub>3</sub>Sn Racetrack Coils Supported by Full-Length and Segmented Shell Structures

Joseph F. Muratore, Giorgio Ambrosio, Michael Anerella, Emanuela Barzi, Rodger Bossert, Shlomo Caspi, D. W. Cheng, John Cozzolino, Daniel R. Dietderich, John Escallier, Sandor Feher, Helene Felice, Paolo Ferracin, George Ganetis, Arup K. Ghosh, Ramesh C. Gupta, A. R. Hafalia, C. R. Hannaford, Piyush Joshi, Paul Kovach, A. F. Lietzke, Wing Louie, Andrew Marone, Al D. McInturff, F. Nobrega, GianLuca Sabbi, Jesse Schmalzle, Richard Thomas, Daniele Turrioni, and Peter Wanderer

**Abstract**—As part of the LHC Accelerator Research Program (LARP) to build a high performance quadrupole magnet with Nb<sub>3</sub>Sn conductor, a pair of 3.6 m-long Nb<sub>3</sub>Sn racetrack coils has been made at Brookhaven National Laboratory (BNL) and installed in two shell-type support structures built by Lawrence Berkeley National Laboratory (LBL). These magnet assemblies have been tested at 4.5 K at BNL to gauge the effect of extended length and prestress on the mechanical performance of the long structure compared to earlier short models. This paper presents the results of quench testing and compares the overall performance of the two versions of the support structure. We also summarize the shell strain measurements and discuss the variation of quench current with ramp rate.

**Index Terms**—LARP, Nb<sub>3</sub>Sn, racetrack, superconducting magnets.

## I. INTRODUCTION

THE first long racetrack coils wound with Nb<sub>3</sub>Sn cable have been manufactured and tested at Brookhaven National Laboratory (BNL). This work is part of a US LHC Accelerator Research Program (LARP) project to ultimately build long, high gradient, cos  $\theta$ -type quadrupole magnets with Nb<sub>3</sub>Sn for a future luminosity upgrade of the LHC. The advantage of using Nb<sub>3</sub>Sn, with its increased critical current, field, and temperature, over the presently used NbTi, is well known; but the ability to wind, react, and support long models of such magnets had not been demonstrated. A series of short (0.3 m long)

subscale magnets (SM Program) has been successfully built and tested by Lawrence Berkeley National Laboratory (LBL) [1]. A short SM-type racetrack magnet SRS01 has also been built and successfully tested at BNL in order to transfer the LBL technology before building the long models at BNL [2], [3]. The motivation for building and testing long racetrack-style magnets is to demonstrate that long Nb<sub>3</sub>Sn coils, significantly longer than the SM series, could be manufactured and operated. In addition, it is important to verify that the shell-based support structure used in the shorter models could also be up-scaled from the short models to the longer versions without adverse length-dependent effects during cooldown and operation. With these goals in mind, two versions of the long racetrack magnet have been tested at BNL using coils fabricated at BNL and support structures supplied by LBL. The first magnet, called LRS01, had a full-length, one piece support shell and it demonstrated a nominal quench plateau of 9596 A, with a maximum quench current of 9663 A, 91% of the calculated short sample prediction  $I_{ss} = 10600$  A, and corresponding to a peak coil field of 11 T [4], [5]. This compared favorably with SRS01 reaching 96%  $I_{ss}$ . Due to high axial stresses, asymmetrical and variable azimuthal stresses, and shell slippage measured in LRS01, a second version with a segmented shell has been built and tested. This paper reports on the quench performance and strain test results for the second magnet, called LRS02, with comparisons to the LRS01 results.

## II. MAGNET DESCRIPTION

A cross section of the LRS01 and LRS02 magnets is shown in Fig. 1, which depicts the coil subassembly and the components of the shell-based support structure. Both magnets used the same pair of 3.6 m long double layer Nb<sub>3</sub>Sn racetrack coils in a common coil configuration [6], and kept the same characteristics as the short model SRS01 as much as possible, but were longer in length. There were 21 turns per layer with the layer transition between the innermost (pole) turns. Each coil was wound continuously around a segmented iron island, enclosed in stainless steel side rails and end shoes, and reacted individually in special fixtures in an argon atmosphere oven. NbTi leads were then soldered to the reacted coils and each coil was vacuum impregnated with epoxy. The coil sets were then clamped together with a minimal gap by two bolted iron pads to

Manuscript received August 26, 2008. First published June 05, 2009; current version published July 15, 2009. This work was supported in part by the US Department of Energy Contract DE-AC02-98CH10886. This manuscript has been authored by Brookhaven Science Associates LLC.

J. Muratore, M. Anerella, J. Cozzolino, J. Escallier, G. Ganetis, A. K. Ghosh, R. C. Gupta, P. Joshi, P. Kovach, W. Louie, A. Marone, J. Schmalzle, R. Thomas, and P. Wanderer are with the Superconducting Magnet Division, Brookhaven National Laboratory, Upton NY 11973, USA (e-mail: muratore@bnl.gov).

G. Ambrosio, E. Barzi, R. Bossert, S. Feher, F. Nobrega, and D. Turrioni are with the Technical Support Division, Fermilab, Batavia IL 60510, USA.

S. Caspi, D. Cheng, D. R. Dietderich, H. Felice, P. Ferracin, A. R. Hafalia, C. R. Hannaford, A. F. Lietzke, and G. Sabbi are with the Accelerator and Fusion Research Division, Lawrence Berkeley Laboratory, Berkeley CA 94720, USA.

A. D. McInturff was with Lawrence Berkeley Lab. He is now with Texas A&M University, College Station, TX 77843, USA.

Color versions of one or more of the figures in this paper are available online at <http://ieeexplore.ieee.org>.

Digital Object Identifier 10.1109/TASC.2009.2018511

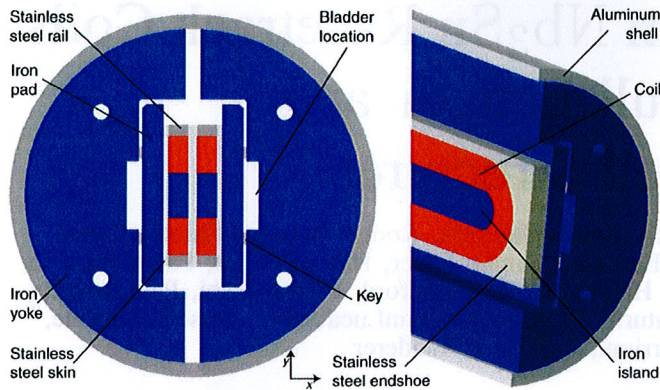


Fig. 1. LRS cross-section (left) and end design (right).

form the coil subassembly, which was then inserted into the support structure, consisting of a laminated iron yoke and 12.7 mm thick aluminum shell with 305 mm outer diameter. Gaps between the pads and yoke allowed the insertion of stainless steel high pressure bladders, which could be pressurized with water to increase separation between pad and yoke so that iron interference keys and shims could be inserted for preloading the coils to the target pre-stresses determined by 3D model computations and data from the short magnet program [5]. Details of the support structure assembly and loading process have been discussed elsewhere [5]. A more detailed description of the coil fabrication, along with cable and strand characteristics, can be found in [4].

### III. MAGNET INSTRUMENTATION

All magnet instrumentation was made from 0.0254 mm thick Type 304 stainless steel foil, bonded onto a 0.0254 mm thick Kapton substrate, and formed into the desired configuration by an etching process to create quench protection heaters, spot heaters, voltage taps, and their connections to the outside, all of which share the limited surface area of the Kapton strip. The quench protection heaters in particular were shaped to provide energy deposition to all turns of all coil surfaces. This composite strip is known as a flexible circuit, or instrumentation trace. Details of the quench protection heater design and the flexible circuit configuration and its successful performance in LRS01 have been described elsewhere [4], [7], [8]. For each of the inner layers, there were three voltage taps on turn 12, where the local field is maximum, for quench propagation studies. Voltage taps were also placed on turns 1 (innermost), 10, 15, and 20. However, the outer layers had taps only on turns 1 and 20. The splices to the leads and the splice between the upper and lower coils were instrumented with taps, as were the transition ramps between layers. Taps were also placed on the superconducting leads and gas-cooled copper leads in order to monitor their voltages during testing.

An analysis of the mechanical behavior of the support structure, performed with a 3D finite element model, showed that the contact friction with the iron laminations prevents the aluminum shell from shrinking longitudinally during cooldown, thus generating an increasing tensional strain in the shell from the ends

towards the center of the magnet [5]. In order to check the numerical predictions, half bridge strain gauges were mounted in 6 stations on each side of the LRS01 shell along the mid plane. Each station included two active gauges, one at axial orientation and one at azimuthal orientation, for a total of 24 active gauges. Each active gauge had an associated “floating” gauge for temperature compensation. The gauges in stations 1 and 2 were used to monitor end effects, whereas the ones in stations 3–6 measured strain variations in the central part of the magnet. Data taken during cool-down confirmed the high tensional strain predicted by the computations [5]. However, when the magnet was ramped to 6000 A for the first time, the shell suddenly slipped axially with respect to the yoke. This was evidenced in the data by a sudden drop in axial tension. The slippage did not induce any quench in the coil. In addition, significant left-right asymmetries and longitudinal variation in the azimuthal strain were observed. In order to reduce the axial strain, improve azimuthal strain uniformity, and demonstrate scalability to longer lengths, it was proposed to segment the shell in 4 sections 0.9 m long and retest the magnet as LRS02.

After the test of LRS01, the magnet was completely disassembled, and the shell segmented and re-instrumented. The shell was again instrumented with half-bridge strain gauges placed on the right side and left side of the magnet mid-plane. The gauges measured the azimuthal and axial strain at 5 stations longitudinally along the shell on each side for a total of 20 active gauges: station 1 was near the lead end and stations 2–5 were at the center of each shell segment. As we will show in the results section, stress/strain uniformity along the length of the structure was significantly improved through the segmentation of the shell, thus resulting in a better mechanical stability.

### IV. EXPERIMENTAL PROCEDURES

LRS02 was tested at the BNL Magnet Division Vertical Test Facility in a 6 m-deep test dewar with a liquid helium bath at an average helium vapor pressure of 1.321 atm, corresponding to a temperature of 4.523 K. Temperatures during testing actually fluctuated from 4.454 K to 4.607 K, as dewar pressure was varied to provide adequate lead cooling flow. Quench tests were performed by ramping the magnet at a specified ramp rate until a quench occurred spontaneously. The standard ramp rate was 20 A/s, but the ramp rate was varied during some tests to measure the effect of eddy current heating. For every ramp, a stop was made at 6000 A to change the quench detector (QD) threshold from 3.6 V to a lower voltage, typically 1.6 V, so as to decrease the time delay between quench start and detection so as to lower the total amount of energy deposited by the quench, as given by the quench integral  $\int [I^2 dt]$  in units of  $10^6 \text{ A}^2 \text{ s}$  (MIITS). The higher threshold before 6000 A was necessary to minimize false QD trips due to the frequent flux jump spikes which occurred during ramps prior to quenches. Such spikes never resulted in a spontaneous quench, but the QD trip caused the quench protection heaters to fire, thus quenching the magnet and resulting in delays needed for cryogenic recovery. For ramps slower than 20 A/s, the rate was 20 A/s until 9000 A, where a stop was made to change to the lower rate. Strain was measured throughout cooldown, testing, and warmup (by taking reads with the strain gauges described above) automatically in

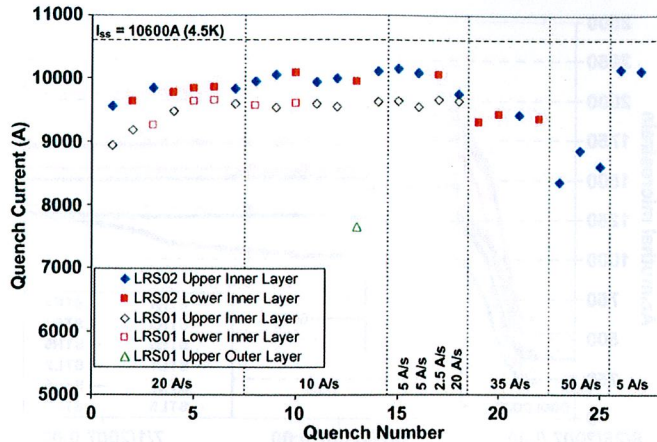


Fig. 2. LRS01 and LRS02 quench history.

the background with control software at intervals of 1–10 minutes, and also at more frequent intervals of 5 s during magnet excitation ramps and specific strain measurement runs.

## V. EXPERIMENTAL RESULTS

### A. Spontaneous Quench Tests

Fig. 2 provides a plot showing all 27 quenches in LRS02 with ramp rates specified. The first 18 quenches of LRS01 (all at 20 A/s) are also included in order to compare the relative performance between the two versions of support structure. As can be seen, there was some training in LRS02 at 20 A/s before it reached a nominal “plateau” of average 9852 A (93%  $I_{ss}$ ), but the quench currents varied over a range of 90 A, 0.9% of the average. This contrasts with LRS01, which at 20 A/s had an average “plateau” of 9596 A (90%  $I_{ss}$ ) and variation of 161 A, 1.7% of average. (The “plateau” averages given are for the 20 A/s quench tests and do not include training quenches or the low outer layer quench in LRS01 that can be seen in the plot.) The highest quench current achieved in LRS02 was 10154 A (96%  $I_{ss}$ ) at 5 A/s, with a computed peak field of 11.50 T. For LRS01, highest reached was 9663 A (91%  $I_{ss}$ ), at 10 A/s. It should be noted that for LRS01, there were no measurable differences of the quench currents among ramp rates of 20 A/s and slower. For LRS02, lower ramp rates resulted in higher quench currents but there was still variation in quench current at each ramp rate. The most variation in quench current for LRS02 was at the 50 A/s “plateau”, where the average of the three quenches at that ramp rate was 8607 A and the range was 509 A, 5.9% of the average. LRS01 at 50 A/s exhibited an average of 8717 A with a range of 247 A, 2.8% of average.

This behavior implies the presence of mechanical motion as the cause of the quenches. Even though there is clear ramp rate dependence in LRS02, continued quench current variation occurs after training at lower ramp rates due to motion generated by the higher Lorentz forces at the higher currents possible with the reduced eddy current heating at the lower ramp rates. There was no correlation between quench current and test temperature variation.

For most quenches in LRS02, the quench started simultaneously in different regions of the magnet, typically in the turn 10

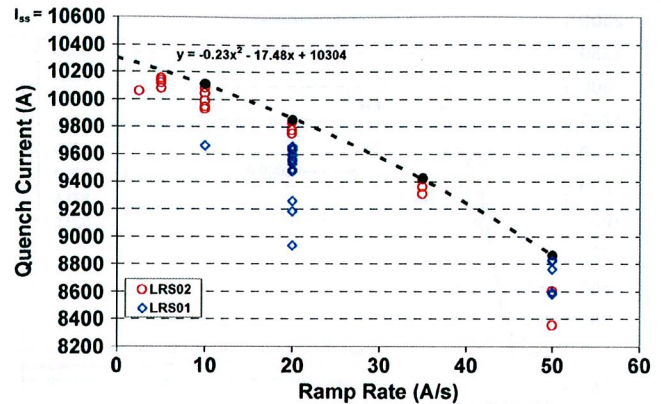


Fig. 3. Quench current vs. ramp rate from 10 A/s to 50 A/s with quadratic fit.

left straight sections and also independently somewhere in turns 12–15. These are regions of high local field. There were a few quenches in the innermost turn and close to the outer turn, areas of lower local field, but these were also accompanied by independent quenching in other parts of the coil. Interestingly, the highest quench of 10154 A at 5 A/s was in an innermost turn, an area of relatively low local field. LRS01 quenches had mostly originated in multiple regions of high local field but there was an outer layer quench in an outermost turn, and there was more variability of locations, with a greater percentage of low field region quenches. In LRS01, 48% of quenches after training were in high field regions. In LRS02, 74% were in high field regions.

As seen in the above results, greater mechanical stability is evident in the performance of LRS02 with the segmented support shell compared to that for LRS01 with the original one piece shell. Nominal plateaus were higher in LRS02 and the maximum quench current increased by 5%. Lower ramp rates resulted in better quench performance due to less eddy current heating, an effect that was not measurable in LRS01 due to its lower quench performance. Most quench origins were located in high field regions in LRS02, but varied much more in LRS01 between high and low field regions.

The highest MIITS value generated was 3.3, corresponding to a hot spot temperature of 160 K, and was from the highest current quench in an innermost (pole) turn. Most quenches generated less than 3 MIITS. As with the previous test of LRS01, the quench protection system of energy extraction and quench protection heaters was able to provide a comfortable margin to the 5 MIITS (300 K) limit of safety [4].

### B. Ramp Rate Study

In order to measure the effects of eddy current heating on quench performance, the magnet was ramped at different rates, as shown in Fig. 3. Since there was variation in quench currents for all ramp rates, the highest current reached for each of the ramp rates of 10, 20, 35, and 50 A/s was plotted as a function of ramp rate, and different fitting curves were used to extrapolate to zero ramp rate, corresponding to no eddy current heating. Linearity of quench current with ramp rate has been observed at the lower ramp rates in previous superconducting magnet testing [9], and a linear fit of the lower ramp rates shows that the extrapolated current is about 10400 A (98%  $I_{ss}$ ) [10], while a quadratic

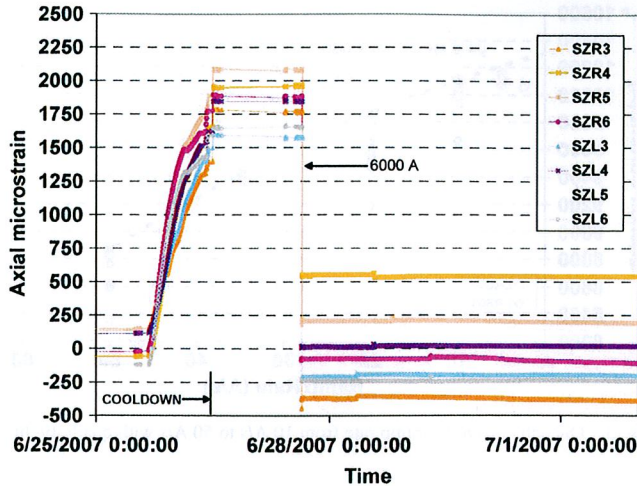


Fig. 4. LRS01 measured axial shell microstrain vs. time during first cool-down and first ramp to 6000 A. Only central stations are plotted (gauge SZL5 appears to be damaged).

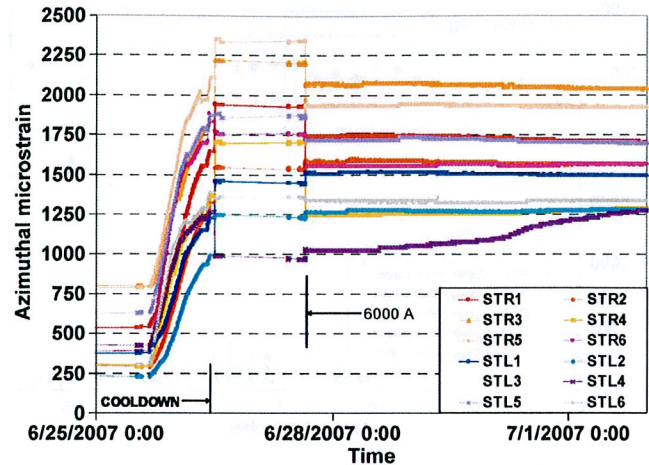


Fig. 6. LRS01 measured azimuthal shell microstrain vs. time during first cool-down and first ramp to 6000 A (gauge STL3 appears to be damaged).

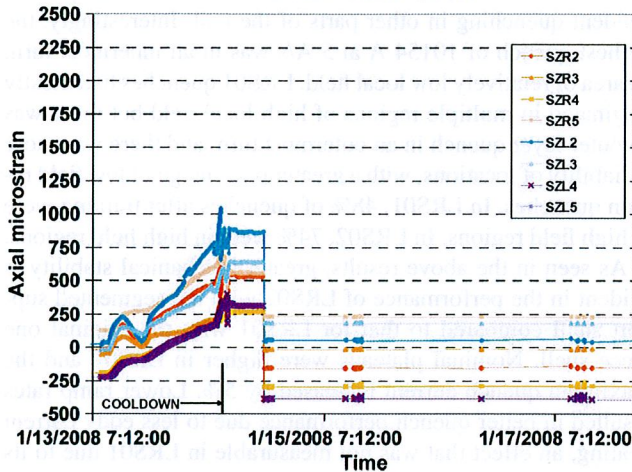


Fig. 5. LRS02 measured axial shell microstrain vs. time during cool-down and test. Only central stations are plotted.

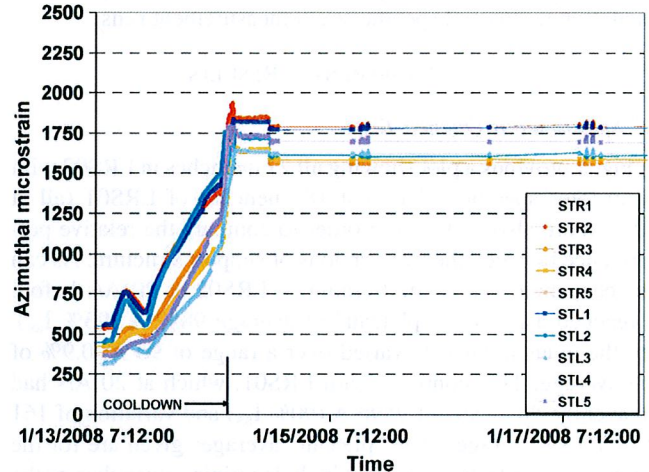


Fig. 7. LRS02 measured azimuthal shell microstrain vs. time during cool-down and test (gauges STR1 and STL4 appear to be damaged).

fit including the 50 A/s data (Fig. 3) give an extrapolated current of 10300 A (97%  $I_{ss}$ ).

### C. Strain Gauge Measurements: LRS01 vs. LRS02

The evolutions of the shell axial strain during cool-down and excitation in LRS01 and LRS02 are shown respectively in Figs. 4 and 5. Only the central stations, where the axial tension is expected to reach its maximum value, are considered (i.e., stations 3 to 6 for LRS01 and stations 2 to 5 for LRS02). During the cool-down of LRS01, the contact friction with the iron laminations prevented the aluminum shell from shrinking longitudinally. As a result, the average axial strain in the central part of the shell increased from  $+44 \pm 110$  microstrain ( $1 \times rms$ ) to  $+1820 \pm 175$  microstrain. When the magnet was ramped to 6000 A for the first scheduled quench-heater test, the shell suddenly slipped axially with respect to the yoke. This was evidenced in the data by a sudden drop in axial strain down to  $-17 \pm 314$  microstrain. In LRS02, the segmentation

of the shell reduced the average strain after cool-down to  $+498 \pm 219$  microstrain. Similarly to LRS01, a slippage of the shell was also recorded in LRS02. Nevertheless, in LRS02 it occurred before the beginning of the first ramp and with the magnet uniformly at a temperature of 4.5 K. Moreover, the resultant drop in axial strain was significantly smaller.

The evolutions of the shell azimuthal strain during cool-down and excitation in LRS01 and LRS02 are plotted respectively in Figs. 6 and 7. All the stations are considered. During the cool-down of LRS01, the average shell azimuthal strain increased from  $+461 \pm 202$  microstrain to  $+1666 \pm 413$  microstrain. In LRS02, the average shell azimuthal strain increased from  $+432 \pm 86$  microstrain to  $+1719 \pm 87$  microstrain, showing that an improvement of the azimuthal strain uniformity along the length has been obtained through the segmentation of the shell. The strain measurements also showed that, during excitation to 10 kA, the electromagnetic forces induced an increase of tensional strain of about 35 microstrain in the shell azimuthal strain [10].

## VI. CONCLUSIONS

The results presented in this report have led to the following important conclusions:

- 1) Magnets made with racetrack-type  $\text{Nb}_3\text{Sn}$  coils and shell-based support structures can be manufactured and perform successfully when extended in length from the short models.
- 2) The segmented shell approach results in improved stress distribution and behavior and better quench performance. (A more detailed explanation of the mechanisms behind this result can be found in [4] but it should be noted that this behavior is not completely understood yet.)

The long racetrack program has thus successfully shown what it set out to do: to demonstrate that long  $\text{Nb}_3\text{Sn}$  magnets can be built and operated with good performance.

## REFERENCES

- [1] A. R. Hafalia *et al.*, "An approach for faster high field magnet technology development," *IEEE Trans. Appl. Supercond.*, vol. 13, no. 2, pp. 1258–1261, June 2003.
- [2] J. Muratore, SRS01 Test Summary BNL Magnet Division Note MDM-653-43, 2007.
- [3] P. Wanderer *et al.*, "LARP long  $\text{Nb}_3\text{Sn}$  racetrack coil program," *IEEE Trans. Appl. Supercond.*, vol. 17, no. 2, pp. 1140–1143, June 2007.
- [4] P. Wanderer *et al.*, "Construction and test of 4 m  $\text{Nb}_3\text{Sn}$  racetrack coils for LARP," *IEEE Trans. Appl. Supercond.*, vol. 18, no. 2, pp. 171–174, June 2008.
- [5] P. Ferracin *et al.*, "Assembly and test of a support structure for 3.6 m long  $\text{Nb}_3\text{Sn}$  racetrack coils," *IEEE Trans. Appl. Supercond.*, vol. 18, no. 2, pp. 167–170, June 2008.
- [6] R. Gupta, "A common coil design for high field 2-in-1 accelerator magnets," in *Proc. 1997 Particle Accel. Conf.*, May 1997, vol. 3, pp. 3344–3346.
- [7] J. Muratore, LRS01 Test Summary BNL Magnet Division Note MDN-654-43, 2008. [Online]. Available: <http://www.bnl.gov/magnets/publications/index.asp>
- [8] H. Felice *et al.*, "Instrumentation and quench protection for LARP  $\text{Nb}_3\text{Sn}$  magnets," presented at the 2008 Appl. Supercond. Conf., Chicago, IL, Aug. 18–22, 2008, Paper 3LPH11, unpublished.
- [9] A. Lietzke, LBL, unpublished data.
- [10] P. Wanderer *et al.*, Test Results of LARP 3.6 m  $\text{Nb}_3\text{Sn}$  Racetrack Coils Supported by Full-Length and Segmented Shell Structures LARP 2008-01-01, February 13, 2008.